JACS
JOURNAL OF THE AMERICAN CHEMICAL SOCIETY
pubs.acs.org/JACS
Article

Taming Highly Enolizable Aldehydes via Enzyme Catalysis for Enantiocomplementary Construction of β-Hydroxyphosphonates

Huangong Li, Zheng Zhu, Dongqi Wu, Yongyuan Ju, Dan Li, Keke Zou, Chaonan Zhu, Jingyu Zhang, Guoliang Zhu, Lixin Zhang, Yonggui Robin Chi, and Yongtao Xie*

Cite This: J. Am. Chem. Soc. 2025, 147, 3102−3109
Read Online
ACCESS | Metrics & More | Article Recommendations | Supporting Information

ABSTRACT: Taming highly enolizable aldehydes for catalytic asymmetric C−C coupling with nucleophiles remains an elusive challenge compared to widely explored simple alkyl or aryl aldehydes. Herein, we use ThDP-dependent enzymes to realize the direct C−C coupling of highly enolizable 2-phosphonate aldehydes with in situ-generated dynamically reversible nucleophiles (acyl anions). Unlike NHC-mediated reactions that yield complex mixtures of multiple adducts, our enzymatic process selectively produces biologically active β-hydroxy phosphonates with high yields (up to 95%) and excellent enantioselectivities (up to 99% ee). The products can be obtained on gram scales and exhibit rich reactivity for downstream transformations to afford diverse molecules. *Pf*BAL (or its mutant A28G) and *Pa*BAL enzymes serve as enantiocomplementary pairs, enabling the synthesis of both product configurations. Mechanistic studies proved that the entrance directions of the active cavities of these two enzyme pairs were distinct, leading to acyl anions formed from these two enzyme pairs attacking 2-phosphonate aldehydes from different orientations.

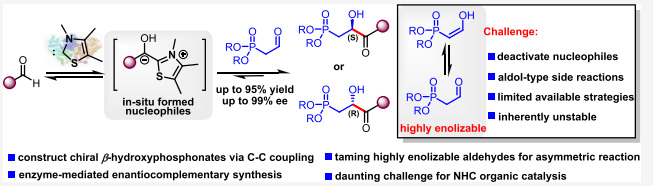

INTRODUCTION

Chiral β-hydroxyphosphonates are unique moieties with a large presence in medicines, agrochemicals, and natural products (Figure 1A).[1] For example, phosphonothrixin, a natural product isolated from *Saccharothrix*, contains a β-hydroxyphosphonate moiety and exhibits herbicidal activity.[1a] Valinophos, a phosphonopeptide natural product, exhibits important antibiotic activity.[1b] Fosfomycin is a widely used antibiotic for treating bacterial infections.[1c] Therefore, the development of an efficient and enantioselective strategy for the construction of β-hydroxyphosphonates is of great interest. Traditional synthetic methods rely on the lipase- or organocatalyst-mediated kinetic resolution of racemic alcohols or esters and afford products with a less than 50% yield (Figure 1B, left).[2] Although reductase or metal-catalyzed reduction of ketophosphonates or vinylphosphonates has been developed, these methods suffer from lengthy routes for substrate preparation (Figure 1B, right).[3] A more attractive approach, based on retrosynthetic analysis, is C−C bond coupling of highly enolizable 2-phosphonate aldehydes with C-nucleophiles (or addition of C-nucleophiles to highly enolizable 2-phosphonate aldehydes) as it uses readily available materials as substrates and offers easily tunable product structures (Figure 1B, down). However, compared with widely explored simple alkyl or aryl aldehydes,[4] taming highly enolizable aldehydes (introducing a strong electron-withdrawing group, such as $-PO_3R$, −COOR, $-NO_2$, $-SO_2R$, etc., to the α-position of aldehyde moieties) for catalytic asymmetric C−C coupling remains an elusive challenge and has been scarcely explored (Figure 1C).[5] The main difficulties are probably attributed to the following factors: (i) the deactivation of common nucleophiles by acidic H at the α-position of aldehyde moieties;[6] (ii) undesirable aldol-type side reactions in the reaction system;[7] (iii) limited catalytic asymmetric strategies;[8] and (iv) the inherent instability of highly enolizable aldehydes.

Herein, we report a ThDP-dependent enzyme-enabled C−C bond coupling reaction between highly enolizable 2-phosphonate aldehydes and nucleophiles, producing biologically active β-hydroxy phosphonates with high yields and excellent chemo- and enantioselectivities (Figure 1D). In this reaction, C-nucleophiles (acyl anions) are catalytically generated in situ from the polarity inversion of another aldehyde, which is mild, dynamically reversible,[9] and compatible with the acidic H-containing 2-phosphonate aldehydes. In addition, the protein cavity of the enzyme catalyst provides subtle noncovalent interactions and molecular recognition, ensuring high reactivity and excellent chemo-/enantioselectivity. Although ThDP-dependent enzymes are well-known for catalyzing benzoin-type C−C couplings between two simple aldehydes,[10] their application to highly enolizable aldehydes remains underexplored despite offering

Received: August 29, 2024
Revised: December 11, 2024
Accepted: January 9, 2025
Published: January 17, 2025

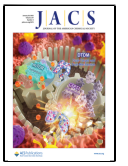

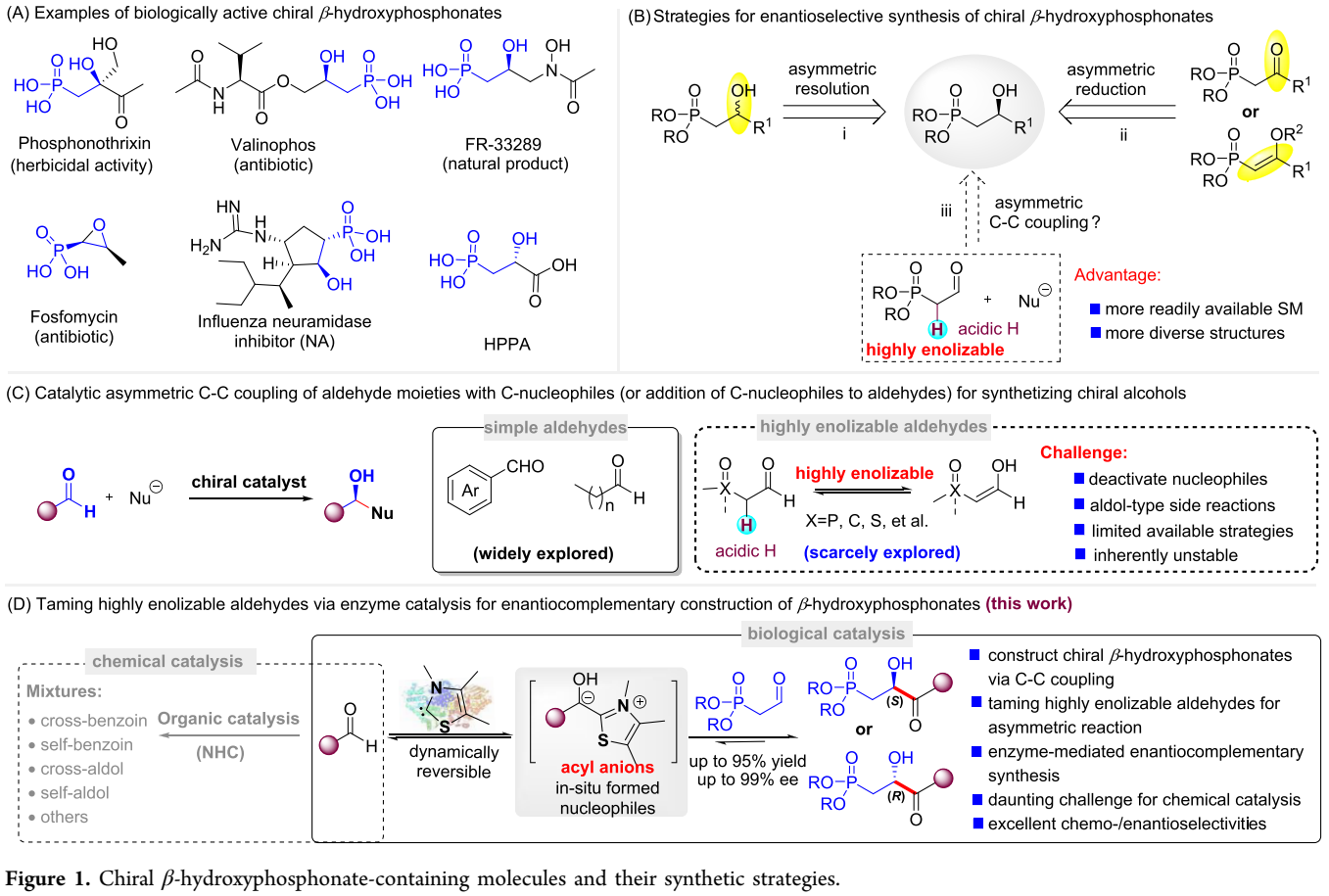

Figure 1. Chiral β-hydroxyphosphonate-containing molecules and their synthetic strategies.

access to hard-to-reach products and facilitating the concise synthesis of complex natural products or medicines.[11] In addition, the synthesis of two mirror-image molecules with ThDP-dependent enzymes is very difficult, owing to the lack of enantiocomplementary enzyme pairs. In 2014, Pohl and co-workers engineered *Ap*PDC to produce (*S*)-benzoins, complementing the (*R*)-benzoins from natural enzymes, but the substrates were limited to aromatic aldehydes.[12] Moreover, only a few substrates have been reported for enantiocomplementary cross-coupling between aromatic aldehydes and simple alkyl aldehydes, typically with low to moderate yields and ee.[10a,13] In this work, *Pf*BAL and *Pa*BAL were demonstrated to be enantiocomplementary ThDP-dependent enzyme pairs, yielding β-hydroxyphosphonates in two configurations. Mechanistic studies proved that the active cavities of the two proteins had distinct entrance directions, leading to acyl anions attacking 2-phosphonate aldehydes in different orientations.

RESULTS AND DISCUSSION

Reaction Development. We initiated our studies by investigating a panel of structurally diverse ThDP-dependent enzymes (cell-free lysates; for phylogenetic analysis, see Figure S2 in the SI) for their ability to catalyze the benzoin-type coupling reaction of **1a** or **1m** with the 2-phosphonate acetaldehyde **2a**. Key results are summarized in Table 1 (see Table S7 in the SI for details). Benzaldehyde lyase from *Pseudomonas fluorescens* (*Pf*BAL, PDB ID: 3D7K) furnished the (*S*)-selective β-hydroxyphosphonate **3a** with 90% yield and 98% ee (entry 10). However, the yield dropped sharply when using the electron-withdrawing-group-substituted **1m** (entry 10). Surprisingly, benzaldehyde lyase from *Polymorphobacter arshaanensis* (*Pa*BAL)[14] yielded **3a** and **3m** with the opposite (*R*)-selective configuration (entry 11), enabling the enantio-

Table 1. Optimization of the Reaction Conditions[a]

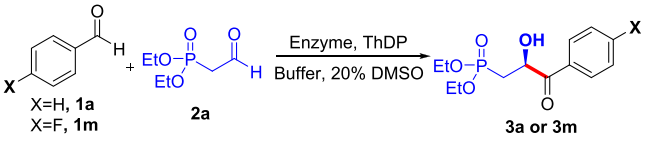

		1a → 3a		1m → 3m	
entry[a]	enzyme	yield (%)[b]	*R*/*S* ratio[b]	yield (%)[b]	*R*/*S* ratio[b]
1	*Ec*Mend	trace		0	
2	*Tp*BFD	trace		0	
3	KdcA	0		0	
4	*Ss*PDC	0		0	
5	*Ec*TK	0		0	
6	*Sc*TK	0		0	
7	*Se*AAS	0		0	
8	*Ss*BAL	10	1:99	trace	
9	*Su*BAL	7	1:99	0	
10	*Pf*BAL	**90**	**1:99**	**10**	**1:99**
11	*Pa*BAL	48	96:4	19	95:5
12	*Pa*BAL (cell)[c]	62	96:4	31	95:5
13	*Pa*BAL (cell)[d]	**85**	**96:4**	60	95:5

[a]Reaction conditions: **1a** or **1m** (0.02 mmol), **2a** (0.04 mmol), cell-free extract (50 mg/mL, 400 μL), ThDP (0.15 mM), $MgSO_4$ (2.5 mM), KPB buffer (50 mM, pH 7.25), DMSO (20% v/v), 1000 rpm, 20 °C, 24 h. [b]Yield and *R*/*S* ratio were determined by chiral HPLC. [c]pH 7.25, whole cell (50 mg/mL). [d]pH 8.0, whole cell (100 mg/mL).

https://doi.org/10.1021/jacs.4c11957
J. Am. Chem. Soc. 2025, 147, 3102−3109

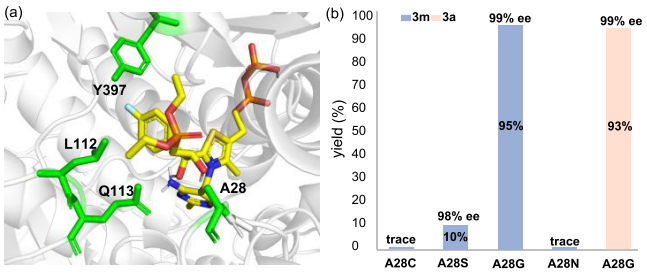

(c)

Enzyme	specific activity (U/mg)	
	3a	3m
*Pf*BAL	3.97	0.09
A28G	5.37	3.47

Figure 2. (a) Molecular docking of the ThDP-bound **3m** precursor. (b) Screening of mutants. (c) Specific activity of *Pf*BAL and A28G.

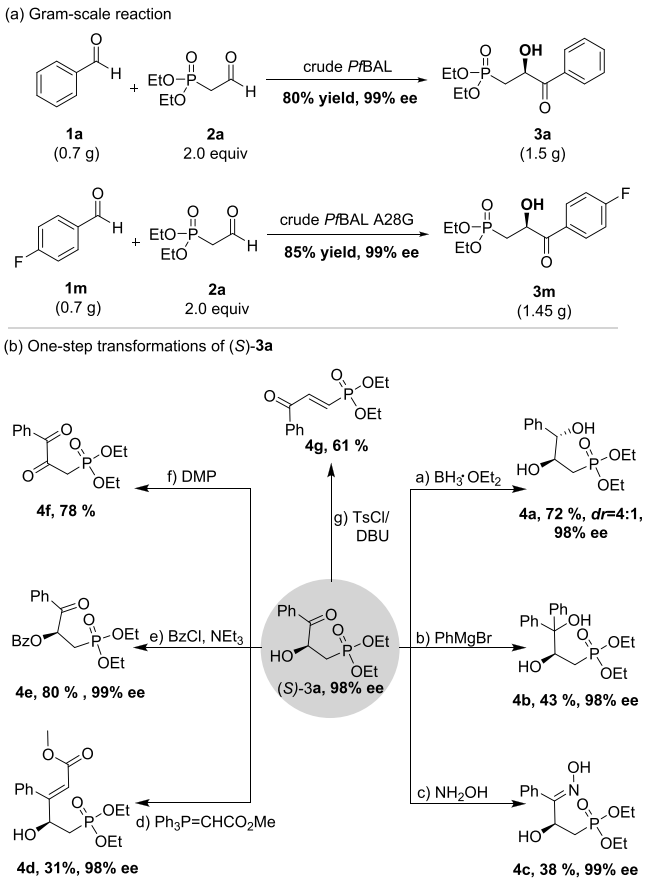

Figure 3. Gram-scale reaction and product transformation.

complementary synthesis of β-hydroxyphosphonates. The yields of **3a** and **3m** were further improved using whole-cell *Pa*BAL and increasing the loading of the enzyme catalyst (entry 13). Subsequently, we focused on engineering *Pf*BAL to enhance the reactivity of substrate **1m** through site saturation mutagenesis (SSM). Molecular docking of the ThDP-bound **3m** precursor with *Pf*BAL identified four key amino acid residues (Y397, L112, Q113, and A28) located within 4 Å of the ThDP-bound **3m** precursor as hot-spots for SSM (Figure 2a). However, no positive mutants were identified when we performed SSM at residues Y397, L112, and Q113, with most mutants exhibiting no catalytic activity (see Tables S11 and S12 in the SI). Surprisingly, the next round of SSM at residue A28 resulted in notable yield improvement using the mutant A28G, producing the desired **3m** in 95% yield and 99% ee (Figure 2b; see Table S11 in the SI for details). Molecular dockings revealed that the attack distance of the **1m**-bound acyl anion intermediate to substrate **2a** in mutant A28G was shorter than that in wild-type *Pf*BAL (4.4 vs 5.8 Å). This may be because the replacement of Ala with Gly at position A28 creates more space for substrate conformational rotation, resulting in a more efficient catalytic conformation (see Figure S3 in the SI). Testing the reactivity of mutant A28G with substrate **1a** also achieved excellent yield and enantioselectivity (93% yield, 99% ee) (Figure 2b). Subsequent specific activity analysis revealed that the mutant A28G showed slightly higher specific activity than *Pf*BAL toward **1a** and a notable improvement of specific activity toward **1m** (Figure 2c), aligning with the yield results. Although four (cross) benzoin products could potentially form, the only byproduct observed was the self-benzoin product of arylaldehydes, with its yield decreased to below 5% (see Tables S7 and S11 in the SI).

Reaction Scope. With the enantiocomplementary enzyme pairs in hand, we then investigated their catalytic scope for the benzoin-type C−C coupling reaction of highly enolizable aldehydes on a preparative scale (Table 2). The results of *Pf*BAL A28G catalysis showed that methyl substituents at the para-, meta-, and ortho-positions of aryl aldehydes were well tolerated, furnishing the corresponding (*S*)-selective products (**3b** to **3d**) with 32−95% yields and excellent ee values. However, the ortho substituent proved to be unreactive for the wild-type *Pf*BAL and *Pa*BAL. Strong electron-donating groups at the phenyl ring of aryl aldehydes, such as hydroxyl or methoxy group, were also well compatible with *Pf*BAL A28G, wild-type *Pf*BAL, and *Pa*BAL (except para-hydroxyl), providing products **3e**−**3g** with excellent yields and ee values. Disubstituted aldehyde afforded the product **3h** with an increased yield for *Pf*BAL A28G compared with wild-type *Pf*BAL. Furthermore, the larger substrate 2-naphthaldehyde failed to yield the corresponding product with wild-type *Pf*BAL, while *Pf*BAL A28G produced **3i** with 85% yield and 97% ee, attributed to the expansion of the active pocket in *Pf*BAL A28G. Both disubstituted aldehyde and 2-naphthaldehyde were suitable substrates for wild-type *Pa*BAL, yielding (*R*)-selective products (**3h** and **3i**, respectively). Although wild-type *Pf*BAL showed good compatibility with various electron-withdrawing groups (such as Br, Cl, and F) at the meta position of aryl aldehydes (**3j** to **3l**), sharply decreased yields were observed for para-substituted electron-withdrawing groups (**3m** to **3q**). However, the mutant A28G was compatible with both meta- and para-substituted electron-withdrawing groups (**3j** to **3q**). Substrates with various electron-withdrawing groups were also suitable for *Pa*BAL (**3j** to **3q**) and showed a better result for substrates with para-substituted electron-withdrawing groups (**3m** to **3q**) compared to wild-type *Pf*BAL and its mutant A28G. The investigation of furan and thiofuran heterocycles (**3r** to **3t**) showed that wild-type *Pf*BAL displayed higher reactivities than *Pf*BAL A28G and *Pa*BAL. Notably, cyano- and pyridine-containing substrates were unreactive under the current reaction conditions (not shown). Next, we tested the compatibility of the other phosphonate substrates. Diisopropoxyphosphate substrates were also well accepted in this benzoin-type coupling process by both mutant A28G and wild-type *Pf*BAL, producing (*S*)-selective products (**3u** to **3w**). *Pa*BAL also yielded (*S*)-selective products (**3u** to **3w**), but with low ee values. We imagine that

https://doi.org/10.1021/jacs.4c11957
J. Am. Chem. Soc. 2025, 147, 3102−3109

Table 2. Substrate Scope[a]

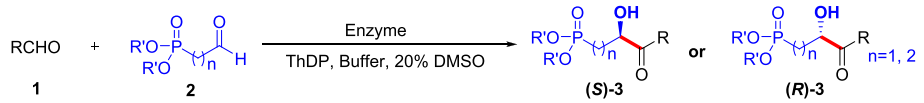

Variation of aromatic aldehydes						
	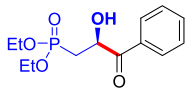 **3a**	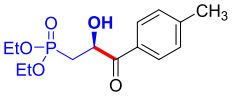 **3b**	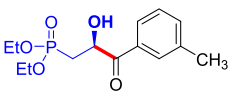 **3c**	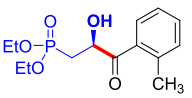 **3d**	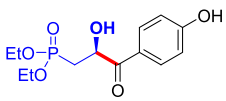 **3e**	
***Pf*BAL:**	91%, 98% ee	77%, 99% ee	85%, 98% ee	0%	88%, 99% ee	**(*S*)**
***Pf*BAL A28G:**	90%, 99% ee	92%, 99% ee	95%, 99% ee	32%, 99% ee	94%, 99% ee	
***Pa*BAL:**	75%, 92% ee	78%, 88% ee	90%, 99% ee	0%	0%	**(*R*)**
	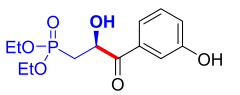 **3f**	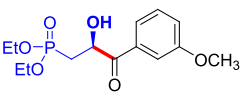 **3g**	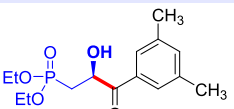 **3h**	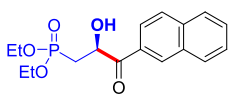 **3i**	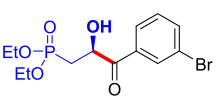 **3j**	
***Pf*BAL:**	80%, 98% ee	91%, 99% ee	50%, 96% ee	0%	80%, 99% ee	**(*S*)**
***Pf*BAL A28G:**	91%, 99% ee	89%, 99% ee	85%, 99% ee	85%, 97% ee	92%, 98% ee	
***Pa*BAL:**	53%, 93% ee	80%, 93% ee	53%, 97% ee	78%, 95% ee	62%, 90% ee	**(*R*)**
	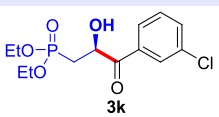 **3k**	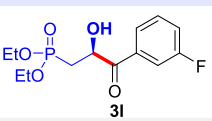 **3l**	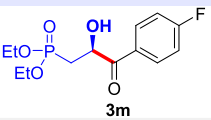 **3m**	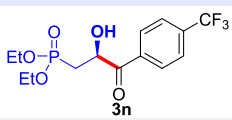 **3n**	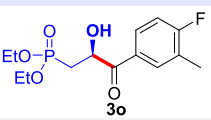 **3o**	
***Pf*BAL:**	85%, 93% ee	92%, 99% ee	13%, 98% ee	trace	0%	**(*S*)**
***Pf*BAL A28G:**	83%, 96% ee	90%, 98% ee	95%, 99% ee	25%, 99% ee	54%, 99% ee	
***Pa*BAL:**	87%, 94% ee	50% (78%)[b], 94% ee	59%, 90% ee	63%, 81% ee	70%, 98% ee	**(*R*)**
	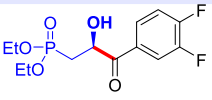 **3p**	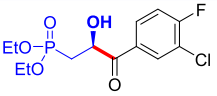 **3q**	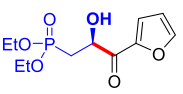 **3r**	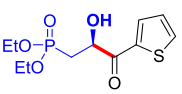 **3s**	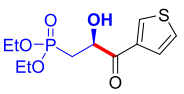 **3t**	
***Pf*BAL:**	0%	0%	90%, 98% ee	87%, 97% ee	83%, 98% ee	**(*S*)**
***Pf*BAL A28G:**	25%, 97% ee	30%, 99% ee	trace	57%, 99% ee	53%, 98% ee	
***Pa*BAL:**	55%, 90% ee	72%, 91% ee	trace	trace	10% (31%)[c], 69% ee	**(*R*)**
Variation of phosphonate moieties						
	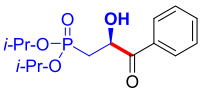 **3u**	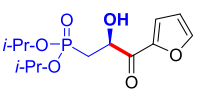 **3v**	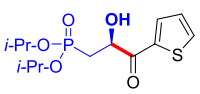 **3w**	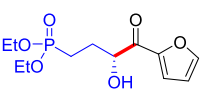 **3x**	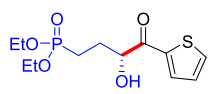 **3y**	
***Pf*BAL:**	65%, 95% ee	78%, 98% ee	74%, 98% ee	75%, 57% ee	52%, 76% ee	**(*S*)**
***Pf*BAL A28G:**	66%, 86% ee	88%, 98% ee	90%, 98% ee	0%	0%	
***Pa*BAL:**	47%, 61% ee	40%, 83% ee	37%, 67% ee	trace	trace	

[a]Reaction condition: **1** (0.15 mmol), **2** (0.3 mmol), cell-free extract for *Pf*BAL and *Pf*BAL A28G (50 mg/mL, 4 mL), whole cell for *Pa*BAL (100 mg/mL, 4 mL), ThDP (0.15 mM), $MgSO_4$ (2.5 mM), KPB buffer (50 mM, pH 7.25 for *Pf*BAL and *Pf*BAL 28G; pH 8.0 for *Pa*BAL), DMSO (20% v/v), 1000 rpm, 20 °C, 24 h; isolate yield. [b]**2a** (2.5 equiv). [c]Whole-cell *Pa*BAL (150 mg/mL).

protein engineering could be used to further invert the enantioselectivity for **3u** to **3w** (see Figure S9 in the SI) and should be applied to phosphate substrates with extended carbon chains (**3x** and **3y**).

Synthetic Applications. To demonstrate the utility of the current method, gram-scale reactions and product transformations were conducted (Figure 3). Both the wild-type *Pf*BAL and its mutant A28G successfully catalyzed the benzoin-type coupling reaction of highly enolizable aldehydes on gram scales, affording the desired products in 80% yield (1.5 g) for **3a** and 85% yield (1.45 g) for **3m** (Figure 3a). Furthermore, the enantioenriched phosphonate product **3a** was easily converted to various derivatives through a one-step reaction (Figure 3b). For instance, the reduction and Grignard reaction of **3a** provided vicinal diol-containing phosphonates **4a** and **4b**. The ketone unit of **3a** was efficiently transformed into imine, producing **4c** with hydroxyl imine. The phosphonate product **3a** also reacted with the Wittig reagent to form alkene **4d** without the loss of ee. In addition, **3a** was easily acylated and oxidized, affording the corresponding

https://doi.org/10.1021/jacs.4c11957
J. Am. Chem. Soc. 2025, 147, 3102−3109

Table 3. Results of NHC Organic Catalysis[a]

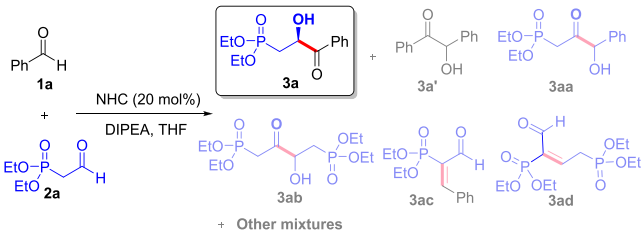

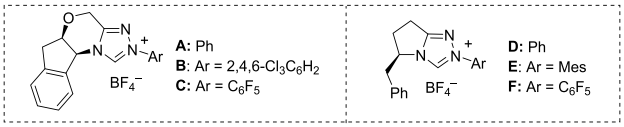

NHC	Conv (%)[b]	3a (%)[c]	ee (%)[d]	3a' (%)[c]	3aa (%)[c]	3ab (%)[c]	3ac	3ad
NHC A	64	0	-	5	5	13	√	√
NHC B	90	14	90	46	8	14	√	√
NHC C	90	8	65	<3	14	<3	√	√
NHC D	42	<3	-	<3	<3	6	√	√
NHC E	46	<3	-	<3	0	0	√	√
NHC F	91	10	27	16	18	17	√	√

[a]Reaction conditions: **1a** (0.15 mmol), **2a** (0.3 mmol), NHC (20 mol %), DIPEA (1.0 equiv) in THF (0.75 mL) at rt for 24 h. [b]Conversion was determined by GC. [c]Yields were determined by GC. [d]ee of **3a** was determined by chiral HPLC; ee of **3a′** and **3ab** was not measured.

products (**4e** and **4f**) in good yields. Finally, the elimination of the hydroxyl group in product **3a** was realized by reacting **3a** with TsCl in the presence of a base. Notably, all of the products derived from **3a** via a one-step reaction could serve as versatile synthetic precursors for further transformations, such as the reduction of imine **4c** or various functionalizations of alkenes **4d** and **4g**.

Comparison with NHC Organic Catalysis. Achieving chemoselective cross-benzoin reactions between two different aldehydes is a classic challenge in synthetic chemistry owing to the presence of three undesirable competing reactions (two homobenzoins and one cross-benzoin).[15] This problem is further complicated when highly enolizable aldehydes are involved as the substrates because of a series of potential side reactions, such as self-/cross-benzoin, self-/cross-aldol reactions, iterative aldol reactions, and the Stetter reaction of aldol products. To demonstrate the unique ability of enzymes to control the chemical selectivity in cross-benzoin reactions involving highly enolizable aldehydes, we conducted the same reaction using different NHC organic catalysts for comparison (Table 3). As speculated, commonly used chiral NHC catalysts **A**–**F** failed to achieve chemoselective cross-benzoin reactions (Table 3). In addition, insufficient conversion, low yields of benzoin-related products, and unsatisfactory stereoselectivities further limited the development of chemoselective cross-benzoin reactions involving highly enolizable aldehydes in NHC organic catalysis. Self- or cross-aldol reactions also appeared in all reaction systems along with other complicated byproducts. These results indicate that avoiding or minimizing competing pathways in cross-benzoin reactions with highly enolizable aldehydes remains a daunting challenge in NHC organic catalysis. In contrast, our enzymatic approach gives unparalleled chemoselective control for this reaction with simultaneous control of the stereochemistry.

Mechanistic Study. To understand the reaction pathway, mechanistic experiments were conducted (Figure 4). Reaction process experiments showed that the benzoin **3a′** (*R* configuration, > 99% ee) formed within 1 h under *Pf*BAL and its mutant A28G catalysis, with *Pf*BAL exhibiting better

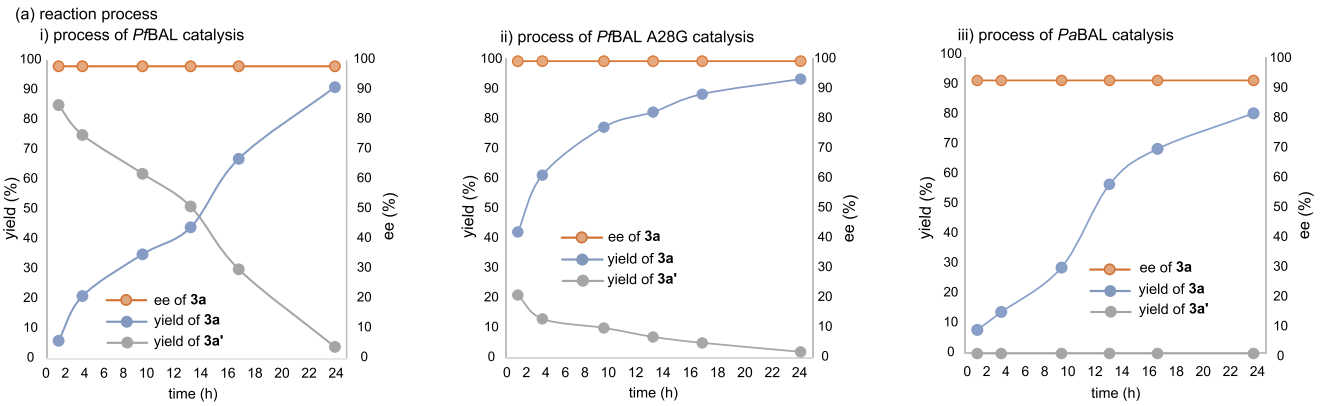

(b) mechanistic experiment

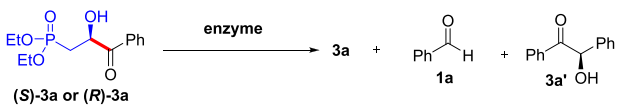

substrate	enzyme	3a (recovery)	1a	3a'
(*S*)-3a	*Pf*BAL	93.0%	3.0%	4.0%
(*S*)-3a	*Pf*BAL A28G	95.0%	3.0%	2.0%
(*R*)-3a	*Pa*BAL	96.0%	4.0%	0%

(c) reaction pathways

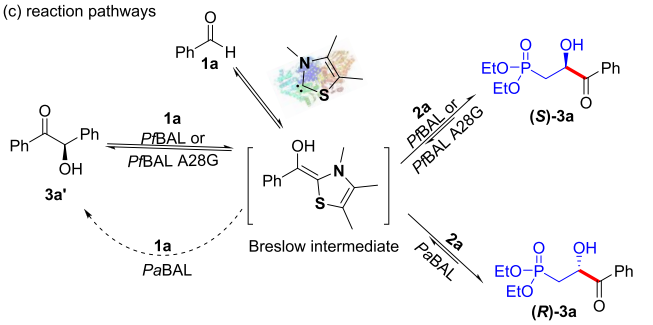

Figure 4. Mechanism-related experiments.

https://doi.org/10.1021/jacs.4c11957
J. Am. Chem. Soc. 2025, 147, 3102−3109

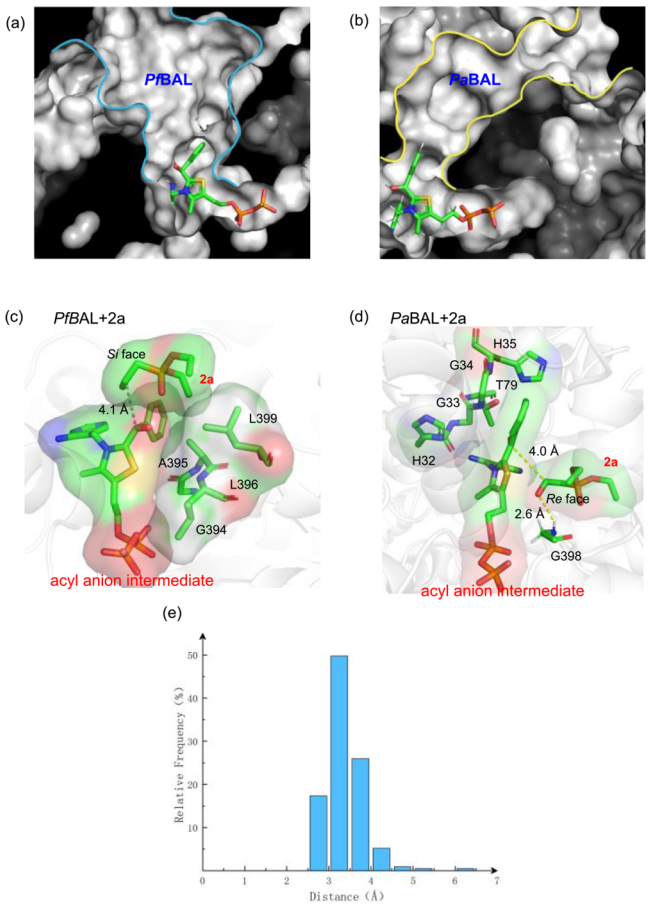

Figure 5. Docking and MD simulations for clarifying the origins of enantioselective complementarity. (a) Active pocket of *Pf*BAL; (b) active pocket of *Pa*BAL; (c) MD simulation for *Pf*BAL; and (d) MD simulation for *Pa*BAL. (e) Relative frequency distribution of the distance between the oxygen atom of **2a** and the hydrogen of the G398 residue. **1a**-bonded acyl anion intermediate, **2a**, and the residue are shown as sticks.

reactivity for producing benzoin **3a′** (Figure 4a,i,ii). Upon prolonging the reaction time, **3a′** was gradually converted into the desired product **3a** under the catalysis of *Pf*BAL or its mutant A28G while maintaining a high level of stereoselectivity. Specific activity analysis demonstrated that the reactivity of natural benzaldehyde was higher than that of unnatural 2-phosphonate aldehyde for *Pf*BAL and *Pf*BAL A28G catalysis (see Table S14 in the SI). These results indicated that the formation of the desired product **3a** through *Pf*BAL and its mutant A28G catalysis involves a dynamically reversible process of benzoin **3a′** formation. Further investigations showed that racemic benzoin or (*R*)-benzoin could also be used as the starting material in our new reaction catalyzed by *Pf*BAL or *Pf*BAL A28G (see Table S15 in the SI). In contrast, no benzoin **3a′** was detected during the formation of the desired product **3a** under *Pa*BAL catalysis (Figure 4a,iii). Next, **3a** was separately exposed to *Pf*BAL, *Pf*BAL A28G, or *Pa*BAL, and benzaldehyde **1a** was detected after 24 h in all experiments (Figure 4b). These results prove that the formation of **3a** and the nucleophilic acyl anion intermediate are also dynamically reversible processes. The dynamically reversible feature of the in situ-generated acyl anion makes it an ideal nucleophile compatible with acidic H-containing 2-phosphonate aldehydes. Built upon these experiments (Figure 4a,b), a postulated reaction pathway is briefly illustrated in Figure 4c.

To clarify the origins of enantioselective complementarity, AlphaFold 2 was employed to predict the structure of *Pa*BAL. We found that the overall structure of *Pa*BAL is strikingly similar to that of *Pf*BAL (Figures S5 and S6 in the SI) despite *Pa*BAL sharing 41% sequence identity with *Pf*BAL based on amino acid sequence alignment (Figure S4 in the SI). Interestingly, the entrance direction of the active cavities in the two proteins is distinct (Figure 5a,b), which may contribute to the different configurations of products. Next, 100 ns molecular dynamic (MD) simulations were conducted using AutoDock vina[16] and Amber24. We found that the acyl anion intermediate in *Pf*BAL attacks the *Si* face of **2a**, yielding the *S* configuration products (Figure 5c). Further analysis of the amino acid residues in the active pocket of *Pf*BAL showed that four residues (G394, A395, L396, and L399) prevented **2a** from reaching the bottom of the acyl anion intermediate to produce the *R* configuration products. In contrast, the *Re* face of **2a** is attacked by an acyl anion intermediate in *Pa*BAL to form *R* configuration products (Figure 5d). It is obvious that there is not enough space on the top of the acyl anion intermediate to accommodate **2a** (to produce the *S* configuration products) in *Pa*BAL due to the appearance of H32, G33, G34, H35, and T79. Notably, a weak hydrogen bond between the G398 residue and **2a** was observed in *Pa*BAL (Figure 5d,e), which also controls the orientation of the aldehyde group in **2a**. These results are consistent with our experimental observations.

CONCLUSIONS

In summary, we have developed a novel C−C coupling system for the enantiocomplementary synthesis of chiral *β*-hydroxyphosphonates. This enzyme-mediated transformation is hard to achieve with small-molecule NHC catalysts owing to the complex mixture of multiple adducts. Diverse control experiments and mechanism studies clarified the reaction pathway and the source of the enantioselective complementarity of *Pf*BAL. The chiral *β*-hydroxyphosphonate products can be obtained on gram scales and exhibit rich reactivities for further downstream transformations, creating additional opportunities for the development of novel C−P drugs.[1] Further studies on the bioactivities of these chiral phosphonates for agricultural and medical applications, as well as the application of this method to the total synthesis of complex natural products, are in progress in our laboratories. Our study offers a new perspective on the C−C coupling of highly enolizable aldehydes with C-nucleophiles (or the addition of C-nucleophiles to highly enolizable aldehydes) and will encourage the further development of new systems to tame highly enolizable aldehydes for asymmetric synthesis.

ASSOCIATED CONTENT

Supporting Information

The Supporting Information is available free of charge at https://pubs.acs.org/doi/10.1021/jacs.4c11957.

Experimental methods; optimization data; protein engineering; details of docking and MD simulations; chemical characterization; and NMR spectra (PDF)

https://doi.org/10.1021/jacs.4c11957
J. Am. Chem. Soc. 2025, 147, 3102−3109

AUTHOR INFORMATION

Corresponding Author

Yongtao Xie − *State Key Laboratory of Bioreactor Engineering, East China University of Science and Technology, Shanghai 200237, China;* orcid.org/0009-0005-2582-1205; Email: ytxie123@ecust.edu.cn

Authors

Huangong Li − *State Key Laboratory of Bioreactor Engineering, East China University of Science and Technology, Shanghai 200237, China*

Zheng Zhu − *State Key Laboratory of Bioreactor Engineering, East China University of Science and Technology, Shanghai 200237, China*

Dongqi Wu − *State Key Laboratory of Bioreactor Engineering, East China University of Science and Technology, Shanghai 200237, China*

Yongyuan Ju − *State Key Laboratory of Bioreactor Engineering, East China University of Science and Technology, Shanghai 200237, China*

Dan Li − *State Key Laboratory of Bioreactor Engineering, East China University of Science and Technology, Shanghai 200237, China*

Keke Zou − *State Key Laboratory of Bioreactor Engineering, East China University of Science and Technology, Shanghai 200237, China*

Chaonan Zhu − *State Key Laboratory of Bioreactor Engineering, East China University of Science and Technology, Shanghai 200237, China*

Jingyu Zhang − *State Key Laboratory of Bioreactor Engineering, East China University of Science and Technology, Shanghai 200237, China*

Guoliang Zhu − *State Key Laboratory of Bioreactor Engineering, East China University of Science and Technology, Shanghai 200237, China*

Lixin Zhang − *State Key Laboratory of Bioreactor Engineering, East China University of Science and Technology, Shanghai 200237, China*

Yonggui Robin Chi − *School of Chemistry, Chemical Engineering, and Biotechnology, Nanyang Technological University, Singapore 637371, Singapore; National Key Laboratory of Green Pesticide, Key Laboratory of Green Pesticide and Agricultural Bioengineering, Ministry of Education, Guizhou University, Guiyang 550025, China;* orcid.org/0000-0003-0573-257X

Complete contact information is available at: https://pubs.acs.org/10.1021/jacs.4c11957

Notes

The authors declare no competing financial interest.

ACKNOWLEDGMENTS

The authors acknowledge the National Natural Science Foundation of China (32301231, 32121005), the East China University of Science and Technology for startup funding (YF0142210), the Fundamental Research Funds for the Central Universities (JKF01231815), the National Key Research and Development Program of China (2020YFA0907200, 2020YFA0907800, 2022YFC2303100, and 2022YFC2303104), the Open Project Funding of the State Key Laboratory of Bioreactor Engineering, and the 111 Project (B18022).

ABBREVIATIONS

MD, molecular dynamics; NHC, *N*-heterocyclic carbene; ThDP, thiamine diphosphate

REFERENCES

(1) (a) Zhu, Y.; Shiraishi, T.; Lin, J.; Inaba, K.; Ito, A.; Ogura, Y.; Nishiyama, M.; Kuzuyama, T. Complete Biosynthetic Pathway of the Phosphonate Phosphonothrixin: Two Distinct Thiamine Diphosphate-Dependent Enzymes Divide the Work to Form a C−C Bond. *J. Am. Chem. Soc.* **2022**, *144*, 16715−19719. (b) Ju, K. S.; Gao, J. T.; Doroghazi, J. R.; Wang, K. K. A.; Thibodeaux, C. J.; Li, S.; Metzger, E.; Fudala, J.; Su, J.; Zhang, J. K.; Lee, J.; Cioni, J. P.; Evans, B. S.; Hirota, R.; Labeda, D. P.; van der Donk, W. A.; Metcalf, W. W. Discovery of Phosphonic Acid Natural Products by Mining the Genomes of 10,000 Actinomycetes. *Proc. Natl. Acad. Sci. U. S. A.* **2015**, *112*, 12175−12180. (c) Grif, K.; Dierich, M. P.; Pfaller, K.; Miglioli, P. A.; Allerberger, F. In Vitro Activity of Fosfomycin in Combination with Various Antistaphylococcal Substances. *J. Antimicrob. Chemoth.* **2001**, *48*, 209−217. (d) Wang, P.-C.; Fang, J.-M.; Tsai, K.-C.; Wang, S.-Y.; Huang, W.-I.; Tseng, Y.-C.; Cheng, Y.-S. E.; Cheng, T.-J. R.; Wong, C.-H. Peramivirphosphonate Derivatives as Influenza Neuraminidase Inhibitors. *J. Med. Chem.* **2016**, *59*, 5297−5310. (e) Huang, J.; Chen, R. An Overview of Recent Advances on the Synthesis and Biological Activity of α-Aminophosphonic Acid Derivatives. *Heteroat. Chem.* **2000**, *11*, 480−492. (f) DeSieno, M. A.; Van der Donk, W. A.; Zhao, H. Characterization and Application of the Fe(II) and α-Ketoglutarate Dependent Hydroxylase FrbJ. *Chem. Commun.* **2011**, *47*, 10025−10027. (g) Horsman, G. P.; Zechel, D. L. Phosphonate Biochemistry. *Chem. Rev.* **2017**, *117*, 5704−5783.

(2) For selected examples, see: (a) Żurawiński, R.; Nakamura, K.; Drabowicz, J.; Kiełbasiński, P.; Mikołajczyk, M. Biocatalytic Syntheses of Chiral Non-Racemic 2-Hydroxyalkanephosphonates. *Tetrahedron: Asymmetry* **2001**, *12*, 3139−3145. (b) Zhang, Y.; Li, Z.; Yuan, C. *Candida Rugosa* Lipase-Catalyzed Enantioselective Hydrolysis in Organic Solvents. Convenient Preparation of Optically Pure 2-Hydroxy-2-Arylethanephosphonates. *Tetrahedron Lett.* **2002**, *43*, 3247−3249. (c) Moriyama, A.; Matsumura, S.; Kuriyama, M.; Onomura, O. Nonenzymatic Kinetic Resolution of Racemic β-Hydroxyalkane Phosphonates with a Chiral Copper Catalyst. *Tetrahedron: Asymmetry* **2010**, *21*, 810−824. (d) Mesas-Sánchez, L.; Díaz-Álvarez, A. E.; Koukal, P.; Dinér, P. Kinetic Resolution of 2-Hydroxy-2-Aryl-Ethylphosphonates by a Nonenzymatic Acylation Aatalyst. *Tetrahedron* **2014**, *70*, 3807−3811.

(3) For selected examples, see: (a) Żymańczyk-Duda, E.; Lejczak, B.; Kafarski, P.; Grimaud, J.; Fischer, P. Enantioselective Reduction of Diethyl 2-Oxoalkylphosphonates by Baker's Yeast. *Tetrahedron* **1995**, *51*, 11809−11814. (b) Wang, Z.; Zeng, Y.; Wu, X.; Li, Z.; Tao, Y.; Yu, X.; Huang, Z.; Chen, F. Access to Chiral α-Substituted-β-Hydroxy Arylphosphonates Enabled by Biocatalytic Dynamic Reductive Kinetic Resolution. *Org. Biomol. Chem.* **2020**, *18*, 2672−2677. (c) Fang, J.; Ren, H.; Xu, S.; Huang, C.; Jiang, Y.; Zhang, W.; You, S.; Qin, B. Asymmetric Synthesis of β-Hydroxyphosphonates via a Chemoenzymatic Cascade. *Org. Lett.* **2024**, *26*, 5458−5462. (d) Vargas, S.; Suárez, A.; Álvarez, E.; Pizzano, A. Highly Enantioselective Hydrogenation of Enol Ester Phosphonates: A Versatile Procedure for the Preparation of Chiral β-Hydroxyphosphonates. *Chem. -Eur. J.* **2008**, *14*, 9856−9859.

(4) (a) Pu, L.; Yu, H.-B. Catalytic Asymmetric Organozinc Additions to Carbonyl Compounds. *Chem. Rev.* **2001**, *101*, 757−824. (b) Yus, M.; González-Gómez, J. C.; Foubelo, F. Catalytic Enantioselective Allylation of Carbonyl Compounds and Imines. *Chem. Rev.* **2011**, *111*, 7774−7854. (c) Holmes, M.; Schwartz, L. A.; Krische, M. J. Intermolecular Metal-Catalyzed Reductive Coupling of Dienes, Allenes, and Enynes with Carbonyl Compounds and Imines. *Chem. Rev.* **2018**, *118*, 6026−6052.

(5) (a) Effenberger, F.; Straub, A. A Novel Convenient Preparation of Dihydroxyacetone Phosphate and Its Use in Enzymatic Aldol Reactions. *Tetrahedron Lett.* **1987**, *28*, 1641−1644. (b) Borisova, S.

A.; Circello, B. T.; Zhang, J. K.; Van der Donk, W. A.; Metcalf, W. W. Biosynthesis of Rhizocticins, Antifungalphosphonate Oligopeptides Produced by Bacillus subtilisATCC6633. *Chem. Biol.* **2010**, *17*, 28−37.

(6) (a) Guanti, G.; Banfi, L.; Zannetti, M. T. Phosphonic Derivatives of Carbohydrates: Chemoenzymatic Synthesis. *Tetrahedron Lett.* **2000**, *41*, 3181−3185. (b) Tobrman, T.; Dvořák, D. Selective Magnesiation of Chloro-Iodopurines: An Efficient Approach to New Purine Derivatives. *Org. Lett.* **2006**, *8*, 1291−1294. (c) Kholod, I.; Vallat, O.; Buciumas, A.-M.; Neels, A.; Neier, R. Synthetic Strategies for the Synthesis and Transformation of Substituted Pyrrolinones as Advanced Intermediates for Rhazinilam Analogues. *Eur. J. Org. Chem.* **2014**, *2014*, 7865−7877.

(7) (a) Trost, B. M.; Brindle, C. S. The Direct Catalytic Asymmetric Aldol Reaction. *Chem. Soc. Rev.* **2010**, *39*, 1600−1632. (b) Yamashita, Y.; Yasukawa, T.; Yoo, W. J.; Kitanosono, T.; Kobayashi, S. Catalytic Enantioselective Aldol Reactions. *Chem. Soc. Rev.* **2018**, *47*, 4388−4480.

(8) Known method by using chiral auxiliary or equivalent chiral metal reagents, see: (a) Zhong, Y.-W.; Dong, Y.-Z.; Fang, K.; Izumi, K.; Xu, M.-H.; Lin, G.-Q. A Highly Efficient and Direct Approach for Synthesis of Enantiopure *β*-Amino Alcohols by Reductive Cross-Coupling of Chiral N-tert-Butanesulfinyl Imines with Aldehydes. *J. Am. Chem. Soc.* **2005**, *127*, 11956−11957. (b) Dinh, M.-T.; Bouzbouz, S.; Péglion, J.-L.; Cossy, J. Synthetic Efforts toward the Synthesis of Octalactins. *Tetrahedron* **2008**, *64*, 5703−5710.

(9) Pareek, M.; Reddi, Y.; Sunoj, R. B. Tale of the Breslow Intermediate, a Central Player in *N*-Heterocyclic Carbene Organo-Catalysis: Then and Now. *Chem. Sci.* **2021**, *12*, 7973−7992.

(10) (a) Müller, M.; Sprenger, G. A.; Pohl, M. C-C Bond Formation Using ThDP-Dependent Lyases. *Curr. Opin. Chem. Biol.* **2013**, *17*, 261−270. (b) Giovannini, P. P.; Bortolini, O.; Massi, A. Thiamine-Diphosphate-Dependent Enzymes as Catalytic Tools for the Asymmetric Benzoin-Type Reaction. *Eur. J. Org. Chem.* **2016**, *2016*, 4441−4459. (c) Ju, Z.; Xu, J.; Li, Z.; Fang, J.; Li, M.; Howell, D. C.; Chen, F. Benzaldehyde Lyase-Catalyzed Enantioselective C−C Bond Formation and Cleavage: A Review. *Green Synth. Catal.* **2022**, *3*, 317−326.

(11) (a) Izquierdo, J.; Hutson, G. E.; Cohen, D. T.; Scheidt, K. A. A Continuum of Progress: Applications of N-hetereocyclic Carbene Catalysis in Total Synthesis. *Angew. Chem., Int. Ed.* **2012**, *51*, 11686−11698. (b) Hernández, K.; Parella, T.; Joglar, J.; Bujons, J.; Pohl, M.; Clapés, P. Expedient Synthesis of C -Aryl Carbohydrates by Consecutive Biocatalytic Benzoin and Aldol Reactions. *Chem. − Eur. J.* **2015**, *21*, 3335−3346. (c) Haghshenas, P.; Gravel, M. Chemo- and Diastereoselective *N*-Heterocyclic Carbene-Catalyzed Cross-Benzoin Reactions Using *N*-Boc-*α*-Amino Aldehydes. *Org. Lett.* **2016**, *18*, 4518−4521. (d) Que, Y.; Shao, H.; He, H.; Gao, S. Total Synthesis of Farnesin through an Excited-State Nazarov Reaction. *Angew. Chem., Int. Ed.* **2020**, *59*, 7444−7449. (e) Parmar, K.; Haghshenas, P.; Gravel, M. Total Synthesis of (+)-Hyacinthacine A1 Using a Chemoselective Cross-Benzoin Reaction and a Furan Photooxygenation-Amine Cyclization Strategy. *Org. Lett.* **2021**, *23*, 1416−1421.

(12) Westphal, R.; Vogel, C.; Schmitz, C.; Pleiss, J.; Müller, M.; Pohl, M.; Rother, D. A Tailor-Made Chimeric Thiamine Diphosphate Dependent Enzyme for the Direct Asymmetric Synthesis of (*S*)-Benzoins. *Angew. Chem., Int. Ed.* **2014**, *53*, 9376−9379.

(13) (a) Müller, M.; Gocke, D.; Pohl, M. Thiamin Diphosphate in Biological Chemistry: Exploitation of Diverse Thiamin Diphosphate-Dependent Enzymes for Asymmetric Chemoenzymatic Synthesis. *FEBS J.* **2009**, *276*, 2894−2904. (b) Hailes, H. C.; Rother, D.; Müller, M.; Westphal, R.; Ward, J. M.; Pleiss, J.; Vogel, C.; Pohl, M. Engineering Stereoselectivity of ThDP-Dependent Enzymes. *FEBS J.* **2013**, *280*, 6374−6394.

(14) Li, Y.; Hu, N.; Xu, Z.; Cui, Y.; Feng, J.; Yao, P.; Wu, Q.; Zhu, D.; Ma, Y. Asymmetric Synthesis of N-Substituted 1,2-Amino Alcohols from Simple Aldehydes and Amines by One-Pot Sequential Enzymatic Hydroxymethylation and Asymmetric Reductive Amination. *Angew. Chem., Int. Ed.* **2022**, *61*, No. e202116344.

(15) (a) Rose, C. A.; Gundala, S.; Connon, S. J.; Zeitler, K. Chemoselective Crossed Acyloin Condensations: Catalyst and Substrate Control. *Synthesis* **2011**, *2011*, 190−198. (b) Gaggero, N.; Pandini, S. Advances in Chemoselective Intermolecular Cross-Benzoin-Type Condensation Reactions. *Org. Biomol. Chem.* **2017**, *15*, 6867−6887. (c) Langdon, S. M.; Wilde, M. D.; Thai, K.; Gravel, M. Chemoselective N-Heterocyclic Carbene-Catalyzed Cross-Benzoin Reactions: Importance of the Fused Ring in Triazolium Salts. *J. Am. Chem. Soc.* **2014**, *136*, 7539−7542.

(16) Trott, O.; Olson, A. J. AutoDock Vina: Improving the Speed and Accuracy of Docking with a New Scoring Function, Efficient Optimization and Multithreading. *J. Comput. Chem.* **2010**, *31*, 455−461.

https://doi.org/10.1021/jacs.4c11957
J. Am. Chem. Soc. 2025, 147, 3102−3109